Optics Letters

Dimensional variation tolerant mode converter/multiplexer fabricated in SOI technology for two-mode transmission at 1550 nm

David Garcia-Rodriguez,* Juan L. Corral, Amadeu Griol, and Roberto Llorente

Nanophotonics Technology Centre, Universitat Politècnica de València, Camino de Vera, s/n, 46022 Valencia, Spain
**Corresponding author: dgarciarodriguez@ntc.upv.es*

Received 23 January 2017; accepted 17 February 2017; posted 27 February 2017 (Doc. ID 284696); published 17 March 2017

The use of an integrated asymmetrical directional coupler for two-mode transmission at 1550 nm is analyzed. The design is based on silicon-on-insulator (SOI) technology and permits mode conversion and mode multiplexing/demultiplexing. In the nominal design, mode conversion and mode (de)multiplexing are achieved with 97% efficiency and a 23.4 dB crosstalk level in the 1540–1560 nm band using a 0.1 μm gap. The dimension tolerance of the SOI process has been taken into account in the selection of the optimum design, and the coupling efficiency would remain above 82.3% (corresponding to 0.8 dB excess loss) with 3σ accuracy. A 90% efficiency has been experimentally obtained.

OCIS codes: (060.1810) Buffers, couplers, routers, switches, and multiplexers; (130.3120) Integrated optics devices; (230.7400) Waveguides, slab; (060.4230) Multiplexing.

https://doi.org/10.1364/OL.42.001221

Recently, significant research efforts have focused on increasing the optical fiber transmission capacity to cope with the rising demand for information transmission. The standard single-mode fiber (SSMF) worldwide deployed operates exclusively in the infra-red band (1.3–1.6 μm). Although the exploitable capacity in the infra-red band is substantial, it shows signs of exhaustion, even when modern modulation schemes are used [1].

Mode-division multiplexing (MDM) is a good solution to overcome the limit on the fiber capacity. New devices such as mode (de)multiplexers to combine and split the modes [2–5] would be required. Different techniques have been proposed to convert and (de)multiplex the modes: for example, liquid crystal on silicon, directional couplers (DCs), asymmetrical directional couplers (ADCs), and long-period fiber Bragg gratings.

ADCs are a compact solution that provide mode conversion and mode (de)multiplexing by exciting the higher order mode from the fundamental one.

Mode conversion is induced by matching the effective index of the higher mode in the wide fiber/waveguide and the effective index of the fundamental mode in the narrow fiber/waveguide [2–11]. ADCs are low loss and cheap devices. The fabrication of ADCs in integrated technology offers lower size, better repeatability, and higher robustness than the fiber-based devices.

Silica-based planar lightwave circuit (PLC) technology has been used to fabricate ADC [5–8], but higher sizes and a higher bending radius (above 5 cm [6]) are required. On the other side, silicon-on-insulator (SOI) technology offers a reduced size and a lower bending radius, which clearly improve the option to integrate several functions on the same chip [9,10]. However, the performance of SOI-based ADCs recently proposed are quite sensitive to dimensional variations, and excess losses around 2 dB or crosstalk levels up to 10 dB should be accepted for waveguide width variations of $\Delta w = \pm 5$ nm $\sim \pm 10$ nm [9]. Unfortunately, size deviations up to ±10 nm are not uncommon in typical SOI technology [12], which would lead to low device yields or high thermal tuning powers.

In this Letter, a comprehensive study of the optimum dimensions for an ADC mode converter and (de)multiplexer in SOI technology is presented. Both the nominal performance of the ADC at the design wavelength and around that wavelength are considered, and the best configuration is selected in terms of the sensitivity to the dimensional variations due to the fabrication accuracy of the state-of-the-art SOI processes. The selected device has been fabricated and measured.

The general concept of the MDM link is depicted in Fig. 1. The system consists of two lasers emitting at 1550 nm propagating the LP_{01} mode in a single-mode fiber (SMF). The two LP_{01} modes are coupled to the SOI mode converter through grating couplers, where they are converted to TE_0 and TE_1 modes and multiplexed to the common output. Both optical signals are then coupled to the two-mode fiber (TMF), corresponding now to the LP_{01} and LP_{11} modes. At the receiver side, the same ADC will be needed to demultiplex each mode to the corresponding photodiode.

The mode converter (Fig. 2) is constructed as an asymmetrical coupler, where the waveguide widths are not equal. The operation principle is regulated by the phase-matching condition, where the effective index of the TE_0 mode in the waveguide A (w_A) must match the effective index of the TE_1 mode

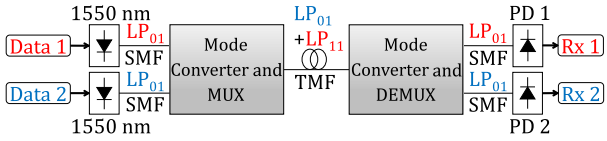

Fig. 1. Scheme for mode-division multiplexing (MDM) at 1550 nm with two-mode fiber (TMF) optical transmission media.

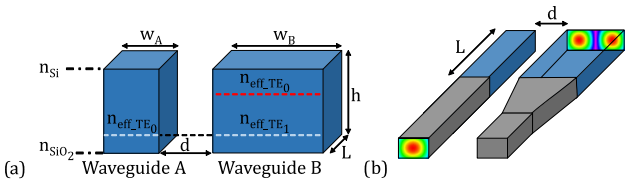

Fig. 2. (a) Refractive index profile for mode coupling between TE_0 and TE_1 modes and (b) a 3D sketch of the mode converter.

in the waveguide B (w_B). The waveguides in the ADC are separated a distance, d, with a certain coupling length, L, and height, h.

According to the coupled-mode theory, the optical fields along each waveguide can be expressed as

$$\vec{E}^A(x,y,z,t) = A(z)\vec{\mathcal{E}}^A_{mn}(x,y)e^{j(\beta^A_{mn}z-\omega t)}, \tag{1}$$

and

$$\vec{E}^B(x,y,z,t) = B(z)\vec{\mathcal{E}}^B_{pq}(x,y)e^{j(\beta^B_{pq}z-\omega t)}, \tag{2}$$

where $\vec{\mathcal{E}}^A_{mn}(x,y)$ y $\vec{\mathcal{E}}^B_{pq}(x,y)$ are the modal profiles of the modes under consideration in each waveguide (mn in the waveguide A and pq in the waveguide B), while β^A_{mn} and β^A_{pq} are the propagation constants for both modes, respectively. The modal profiles and propagation constants correspond to the isolated waveguide modes, whereas the influence of the local modal profiles will be considered in the variation of the complex envelopes, $A(z)$ and $B(z)$, along the direction of propagation.

Assuming L is the length of the directional coupler, if only one mode is present at the waveguide A input of the coupler ($B(0) = 0$), the optical power in both outputs (direct (A) and coupled (B) paths) as a function of the input power P_a (0) is [13]

$$\frac{P_a(L)}{P_a(0)} = \left|\frac{A(L)}{A(0)}\right|^2 = \left(\frac{\kappa_{ab}\kappa_{ba}}{\beta_c^2}\right)\cos^2(\beta_c L) + \left(\frac{\delta}{\beta_c}\right)^2, \tag{3}$$

$$\frac{P_b(L)}{P_a(0)} = \left|\frac{B(L)}{A(0)}\right|^2 = \frac{|\kappa_{ba}|^2}{\beta_c^2}\sin^2(\beta_c L), \tag{4}$$

$$\delta = \frac{(\beta^B_{pq} + \kappa_{bb}) - (\beta^A_{mn} + \kappa_{aa})}{2}, \tag{5}$$

$$\beta_c = \sqrt{\kappa_{ab}\kappa_{ba} + \delta^2}, \tag{6}$$

where κ_{aa} and κ_{bb} are the self-coupling coefficients that take into account the variation in the propagation constant of each mode due to the perturbation caused by the other waveguide; κ_{ab} and κ_{ba} are the mutual coupling coefficients of the waveguide B to A and vice versa which depend on the fiber separation, d; and δ is the phase mismatch. Finally, the coupling efficiency is defined as

$$\eta = \frac{P_b(L)}{P_a(0)} = \frac{|\kappa_{ba}|^2}{\beta_c^2}\sin^2(\beta_c L). \tag{7}$$

Therefore, the optical power is periodically exchanged between both waveguides appearing at the first maximum in the coupled output for a distance:

$$L_c = \frac{\pi}{2\beta_c}. \tag{8}$$

The power transfer will be maximized when the phase-matching condition is fulfilled ($\delta = 0$), which implies that the propagation constants of both modes in the coupler have to be the same and, therefore, the refractive indices will also be equal.

When the coupler is made of similar waveguides (DC), the phase match condition is always fulfilled if the modes to be coupled are the same one (A = B), regardless of the wavelength. However, in an ADC, the effective indices of the modes to be coupled, which are wavelength dependent, must be matched by properly selecting the dimensions of the respective waveguides to be used.

A silicon-on-insulator wafer with a silicon thickness of 220 nm has been selected for the design of the coupler, as it has become the standard substrate for several established research and development foundries [12]. The refractive indices of Si and SiO_2 are $n_{Si} = 3.47$ and $n_{SiO_2} = 1.46$, respectively, and the eigenmodes' effective indices in the waveguides will be calculated with the three-dimensional (3D) beam propagation method (3D-BPM). For this height, the TE polarization has lower bending losses [12].

ADC is made of a single-mode waveguide propagating the TE_0 mode and a two-mode waveguide propagating both TE_0 and TE_1 modes. TE_0 enters the single-mode waveguide, and it is converted to TE_1 in the two-mode waveguide. The width of the single-mode waveguide is taken as $w_A = 0.45$ μm with an effective index value of $n_{\text{eff\_TE}_0} = 2.4109$ at 1550 nm. The effective index of TE_0 in the single-mode waveguide must match the TE_1 in the two-mode waveguide which can be accomplished by increasing the width of the two-mode waveguide up to $w_B = 0.962$ μm. For this width, the effective index values are $n_{\text{eff\_TE}_0} = 2.7390$ and $n_{\text{eff\_TE}_1} = 2.4106$.

TE_0 to TE_1 coupling efficiency and TE_0 insertion losses are the most important parameters to evaluate the performance of the ADC as mode converter and multiplexer. Due to the effective index difference, both TE_0 modes do not interact, and the TE_0 insertion losses in the two-mode waveguide are negligible.

The ADC has been simulated at 1550 nm for different gap, d (μm), and coupling length, L (mm), values. The coupling efficiency results are depicted in Fig. 3, where it is shown that for any given gap value the maximum coupling efficiency is achieved for different coupling lengths, according to Eq. (7).

For wider gaps between the waveguides, the mutual coupling coefficients are reduced and, therefore, the ADC requires longer coupling lengths to achieve the maximum coupling efficiency.

Different gap/length combinations have been selected in order to compare the performance of the ADC around 1550 nm and its robustness against fabrication tolerances. The four cases are highlighted in Fig. 3 and correspond to these dimensions: ($d = 0.1$ μm, $L_1 = 12.62$ μm), ($d = 0.1$ μm, $L_2 = 38.10$ μm),

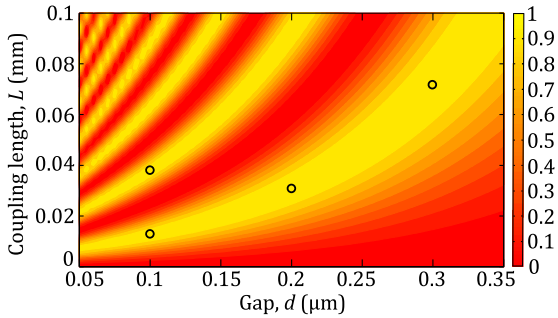

Fig. 3. Coupling efficiency from TE_0 to TE_1 for an asymmetrical directional coupler with the refractive index profile from Fig. 2.

($d = 0.2$ μm, $L = 30.98$ μm), and ($d = 0.3$ μm, $L = 72.08$ μm).

When the ADC acts as a mode demultiplexer, both TE_0 and TE_1 modes enter the two-mode waveguide, and each mode should exit the coupler from different outputs. (TE_0 remains in the two-mode waveguide, whereas the TE_1 is converted to TE_0 in the single-mode output.) In addition to the previously considered parameters, the crosstalk between both outputs is the most important parameter to assess; namely, the extinction ratio of the TE_1 mode in the two-mode waveguide and the undesired leakage of the TE_0 mode to the single-mode waveguide.

If the performance of all ADC parameters is considered both at 1550 nm and its evolution around the design wavelength, the optimum dimensions of all four selected cases are slightly modified as ($d = 0.1$ μm, $L_1 = 12.50$ μm), ($d = 0.1$ μm, $L_2 = 37.74$ μm), ($d = 0.2$ μm, $L = 30.74$ μm), and ($d = 0.3$ μm, $L = 70.92$ μm). The coupling efficiency associated with these four cases is depicted in Fig. 4(a), where the wavelength dependence of the effective modal indices is also considered in the simulations. These results show that all cases offer an efficiency better than 97.4% at 1550 nm. If a 20 nm bandwidth around the design wavelength is considered, the best performance in terms of coupling efficiency is obtained for a 0.2 μm gap ($L = 30.74$ μm) with a 98.7% coupling efficiency (corresponding to 0.06 dB excess loss), compared

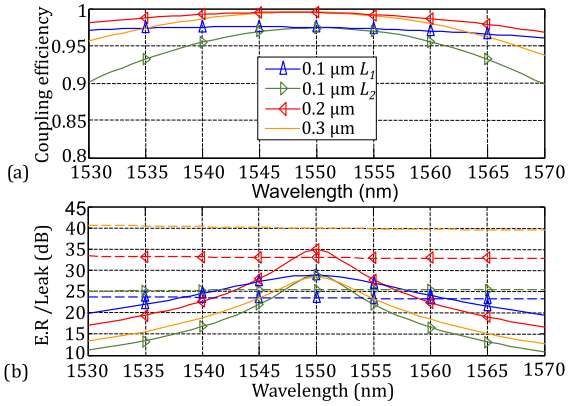

Fig. 4. (a) Coupling efficiency from TE_0 to TE_1 and (b) TE_1 extinction ratio and TE_0 leakage (dashed line) for the asymmetrical directional coupler from Fig. 2 for different combinations of gap, d, and coupler length, L.

to 97% for a 0.1 μm gap. From the results in Fig. 4(a), it can be stated that for any given gap distance the shortest length offering the maximum coupling should be selected, as the ($d = 0.1$ μm, $L_2 = 37.74$ μm) case is quite a bit more wavelength sensitive than the ($d = 0.1$ μm, $L_1 = 12.50$ μm) case. For all three cases, with the shortest length, the coupling efficiency in C band is better than 95.5% or 0.2 dB excess loss.

In Fig. 4(b), it can be seen that all four cases have TE_1 extinction ratio levels better than 28.4 dB at 1550 nm and as high as 34.7 dB for the best configuration. However, the TE_1 extinction ratio is quite sensitive to wavelength variation, and the best performance is obtained for the ($d = 0.1$ μm, $L_1 = 12.50$ μm) case where an extinction ratio better than 24.2 dB is achieved in a 20 nm range around 1550 nm. From this figure, it can be stated that the wider the gap between both waveguides, the lower the TE_1 extinction ratio in a certain bandwidth around the design wavelength.

In terms of the TE_0 leakage, the results from Fig. 4(b) show that the lowest leakage is obtained when the waveguides are further separated, as could be expected due to the highest confinement of this mode. The TE_0 leakage dependence on the wavelength is quite low, and a level better than 23.4 dB is obtained on a 20 nm bandwidth. All in all, the best performance in terms of crosstalk is obtained for the ($d = 0.1$ μm, $L_1 = 12.50$ μm) case. A narrower gap would impair further the TE_0 crosstalk level. If the results for both cases with a $d = 0.1$ μm gap are compared, the case with a shortest length offers again the best results.

In terms of the nominal design, all four cases offer an outstanding performance as mode converter and mode multiplexer/demultiplexer at the design wavelength. When a certain bandwidth is considered, the shortest coupling length for any given gap separation is always preferred. In these cases, there are some minor differences between the three gap values analyzed, and the selection of the best design will depend on which parameter (coupling efficiency, TE_1 extinction ratio or TE_0 leakage) is considered to be the most critical for the application.

We will now take into account the tolerances of the fabrication process in terms of waveguide width variations. We will consider a SOI CMOS-compatible process based on a 193 nm optical deep UV dry lithography and dry etching for 200 mm wafers as a typical process to be found in fabrication foundries. The 3σ accuracy of the linewidth uniformity for this process has been found to be ±8 nm [11]. Thus, the waveguide dimensions of the ADCs can be estimated to fulfill these accuracies with a 99.7% probability.

The ADC configurations previously selected have been simulated for w_A and w_B waveguide widths, ranging from 0.43 to 0.47 μm and 0.94 to 0.98 μm, respectively. The sensitivity of the coupling efficiency to these width variations is shown in Fig. 5 for all four gap/length combinations previously selected. It can be seen that the best configuration in terms of coupling efficiency (0.2 μm gap), according to the nominal widths, offers a less robust design than the configurations with a narrower gap, $d = 0.1$ μm. Using a 0.1 μm gap instead of the 0.2 μm one implies that a shorter coupling length is needed. Therefore, any changes in the waveguide dimensions and, consequently, in the propagation constants, will affect to a lesser extent the coupling efficiency when Eq. (7) is considered.

In fact, Fig. 5(a) shows a region where the efficiency coupling remains quite high if the variation in the widths is within

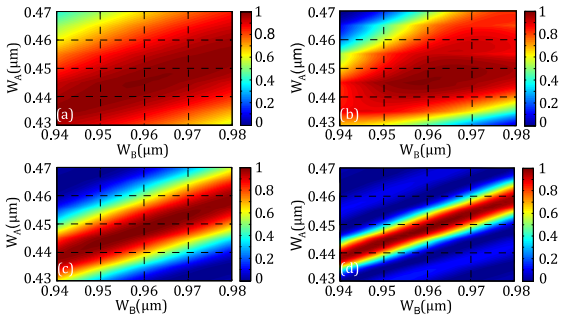

Fig. 5. Sensitivity of TE_0 to TE_1 coupling efficiency to the variation of the waveguide widths. (a) 0.1 μm L_1, (b) 0.1 μm L_2, (c) 0.2 μm, and (d) 0.3 μm.

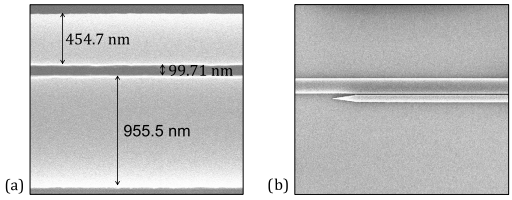

Fig. 6. SEM image. (a) w_A, w_B and *gap* values and (b) coupling zone.

±8 nm, obtaining an efficiency above 82.3% or 0.8 dB excess loss.

However, when the gap between waveguides is 0.2 and 0.3 μm, the same width variation would imply quite a reduction in the coupling efficiency, obtaining minimum values around 46% and 0%, respectively. An interesting result from Fig. 5 is that the coupling efficiency is at its maximum and remains constant when the width variations are proportional in both waveguides. If the variation of the coupling efficiency along any of the axes is compared, it can be seen that the accuracy of the width of the single-mode waveguide is more critical than the variation of the width for the wide waveguide.

In order to test the thermal sensitivity of the ADC, the silicon thermo-optic coefficient ($1.86 \cdot 10^{-4}$ K^{-1}) has been considered in the simulations, and a coupling efficiency variation below 0.2% has been obtained when a ±20 K temperature range is considered.

The ADC with a 0.1 μm gap has been fabricated in the NTC laboratory with a SOI CMOS-compatible process based on an E-beam lithography [14]. The device is made of two independent single-mode waveguides (width w_A) coupled through an intermediate two-mode waveguide (width w_B) so a double TE_0-TE_1 and TE_1-TE_0 coupling would take place. Both input and output single-mode waveguides are vertically coupled to an SSMF fiber by means of grating couplers. In order to avoid any undesirable reflection, the waveguides were tapered after the coupling zone, as shown in Fig. 6(b), and the coupling length (straight zone) was reduced to $L = 12.30$ μm to take into account the additional coupling within the tapered waveguides. The measurement results for this device show that the experimental coupling efficiency has a similar response to the theoretical one at the 1530–1570 nm band. The

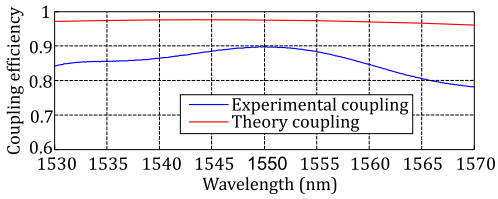

Fig. 7. Theoretical and experimental conversion efficiency from the TE_0 to TE_1 mode for a 0.1 μm gap.

experimental coupling efficiency is 90% at 1550 nm, 7.5% below the theoretical coupling, corresponding to an additional 0.35 dB excess loss. If a 20 nm bandwidth around the design wavelength is considered, the experimental coupling is higher than the 84%, as is shown in Fig. 7. The small differences between theoretical and experimental coupling are due to waveguide and gap variations in the fabrication process, as can be seen in Fig. 6(a).

Figure 6 shows a SEM image of the fabricated sample. In Fig. 6(a), which is a zoomed area from Fig. 6(b), it is possible to see the actual dimensions of the waveguide widths and the coupling gap in the coupling zone. According to Fig. 5(a), the achieved dimension variations shown in Fig 6(a) will correspond to an efficiency of 90% at 1550 nm, similar to the measured value. If the same error had occurred in the 0.2 and 0.3 μm gap devices, the efficiency would be around 60% and 20%, respectively.

Funding. Ministerio de Economía y Competitividad (MINECO) (TEC2015-70858-C2-1-R, RTC-2014-2232-3).

REFERENCES

1. J. J. Benson, Jr., S. Spaelte, and M. V. Shastri, in *Optical Fiber Communication Conference and National Fiber Optic Engineers Conference*, Anaheim, California, USA, 2013, paper OTh4B.7.
2. T. Uematsu, K. Saitoh, N. Hanzawa, T. Sakamoto, T. Matsui, K. Tsujikawa, and M. Koshiba, in *Optical Fiber Communication Conference and National Fiber Optic Engineers Conference*, Anaheim, California, USA, 2013, paper OTh1B.5.
3. M. Greenberg and M. Orenstein, Opt. Express **13**, 9381 (2005).
4. T. Uematsu, Y. Ishizaka, Y. Kawaguchi, K. Saitoh, and M. Koshiba, J. Lightwave Technol. **30**, 2421 (2012).
5. Y. H. Ding, J. Xu, F. D. Ros, B. Huang, H. Y. Ou, and C. Peucheret, Opt. Express **21**, 10376 (2013).
6. N. Hanzawa, K. Saitoh, T. Sakamoto, T. Matsui, K. Tsujikawa, M. Koshiba, and F. Yamamoto, Opt. Express **22**, 29321 (2014).
7. N. Hanzawa, K. Saitoh, T. Sakamoto, T. Matsui, K. Tsujikawa, M. Koshiba, and F. Yamamoto, Opt. Express **21**, 25752 (2013).
8. N. Hanzawa, K. Saitoh, T. Sakamoto, T. Matsui, K. Tsujikawa, T. Uematsu, and F. Yamamoto, J. Lightwave Technol. **33**, 1161 (2015).
9. J. Wang, S. He, and D. Dai, Laser Photon. Rev. **8**, L18 (2014).
10. D. Dai, J. Wang, and Y. Shi, Opt. Lett. **38**, 1422 (2013).
11. J. L. Corral, D. Garcia-Rodriguez, and R. Llorente, IEEE Photon. Technol. Lett. **28**, 425 (2016).
12. D. X. Xu, J. H. Schmid, G. T. Reed, G. Z. Mashanovich, D. J. Thomson, M. Nedeljkovic, X. Chen, D. Van Thourhout, S. Keyvaninia, and S. K. Selvaraja, IEEE J. Sel. Top. Quantum Electron. **20**, 422 (2014).
13. J. M. Liu, *Photonic Devices* (Cambridge University, 2007).
14. A. E. Grigorescu, M. C. van der Krogt, and C. W. Hagen, Proc. SPIE **6519**, 65194A (2007).